# $P2Y_{12}$ receptor modulation of ADP-evoked intracellular $Ca^{2+}$ signalling in THP-1 human monocytic cells

Micklewright JJ[1], Layhadi JA[1] and Fountain SJ[1,2]

[1]Biomedical Research Centre, School of Biological Sciences, University of East Anglia

[2]Correspondence: Samuel J Fountain,

Running title: $P2Y_{12}$ modulates ADP signalling in monocytes

## ACKNOWLEDGEMENTS

This work was supported by the BBSRC.

## ABSTRACT AND KEYWORDS

### Background and purpose

The $G_i$-coupled, ADP-activated $P2Y_{12}$ receptor is well characterised as playing a key role in platelet activation via crosstalk with $P2Y_1$ in ADP-evoked intracellular $Ca^{2+}$ response. There is limited knowledge on the role of $P2Y_{12}$ in ADP-evoked $Ca^{2+}$ responses in other blood cells. Here we investigate the role of $P2Y_{12}$ receptor activation in modulation of ADP-evoked $Ca^{2+}$ responses in human THP-1 monocytic cells.

### Experimental approach

A combination of intracellular $Ca^{2+}$ measurements, RT-PCR, immunocytochemistry, leukocyte isolation and siRNA-mediated gene knockdown were used to identify the role of $P2Y_{12}$ receptor activation.

### Key results

ADP-evoked intracellular $Ca^{2+}$ responses ($EC_{50}$ 2.7 μM) in THP-1 cells were abolished by inhibition of phospholipase C (U73122) or sarco/endoplasmic reticulum $Ca^{2+}$-ATPase (thapsigargin). Loss of ADP-evoked $Ca^{2+}$ responses following treatment with MRS2578 ($IC_{50}$ 200 nM) revealed a major role for $P2Y_6$ in mediating ADP-evoked $Ca^{2+}$ responses. ADP-evoked responses were attenuated either with pertussis toxin treatment, or $P2Y_{12}$ inhibition with two chemically distinct antagonists (ticagrelor, $IC_{50}$ 5.3 μM; PSB-0739, $IC_{50}$ 5.6 μM). ADP-evoked responses were suppressed following siRNA-mediated $P2Y_{12}$ gene knockdown. The inhibitory effects of $P2Y_{12}$ antagonists were fully reversed following adenylate cyclase inhibition (SQ22536). $P2Y_{12}$ receptor expression was confirmed in freshly isolated human $CD14^+$ monocytes.

### Conclusion and implications

Taken together, these data suggest that $P2Y_{12}$ activation positively regulates $P2Y_6$-mediated intracellular $Ca^{2+}$ signalling through suppression of adenylate cyclase activity in human monocytic cells.

This article has been accepted for publication and undergone full peer review but has not been through the copyediting, typesetting, pagination and proofreading process which may lead to differences between this version and the Version of Record. Please cite this article as doi: 10.1111/bph.14218

**Abbreviations:** adenosine 5'-diphosphate (ADP); phospholipase C (PLC); inositol 1,4,5-triphosphate ($IP_3$); phosphatidylinositol 4,5-bisphosphate ($PIP_2$), cyclic adenosine monophosphate (cAMP); phosphatidylinositol-3-kinase (PI3K); uridine diphosphate (UDP); protein kinase A (PKA).

**Keywords:** Purinergic, ADP, monocyte, P2Y receptor, calcium signalling

## INTRODUCTION

The adenine nucleotide ADP serves as an important signalling molecule that is implicated in processes such as platelet aggregation (Dorsam and Kunapuli, 2004) and immune modulation (Ben Addi et al., 2010). ADP binds to $P2Y_1$, $P2Y_6$, $P2Y_{12}$ and $P2Y_{13}$, which are members of the G protein-coupled P2Y receptor family. Activation of Gq-coupled $P2Y_1$ and $P2Y_6$ causes downstream $IP_3$ generation via PLC-mediated breakdown of $PIP_2$, and subsequent calcium ion ($Ca^{2+}$) release through endoplasmic reticulum $IP_3$ receptors (Erb and Weisman, 2012). Conversely, $P2Y_{12}$ and $P2Y_{13}$ are $G_i$-coupled and hence inhibit production of cAMP and stimulate PI3K when activated (Erb and Weisman, 2012).

Platelet aggregation in response to ADP is one of the earliest examples of extracellular nucleotide signalling. It is firmly established that ADP activates platelets via the $P2Y_1$ and $P2Y_{12}$ receptors, and the functionality of both receptors is required for normal platelet aggregation (Jin and Kunapuli, 1998). The emergence of $P2Y_{12}$ as a vital component in ADP-evoked platelet activation has led to the development of anti-platelet drugs targeting this receptor, such as ticagrelor and clopidogrel. The rise in cytosolic $Ca^{2+}$ in response to ADP is deemed responsible for the ADP-mediated activation of platelets (Dorsam and Kunapuli, 2004). Although $P2Y_{12}$ is $G_i$-coupled and should therefore not cause intracellular $Ca^{2+}$ mobilisation, outcomes from a previous study suggest that $P2Y_{12}$ potentiates the $G_q$ $P2Y_1$-mediated $Ca^{2+}$ response to ADP in a cross-talk mechanism (Hardy et al., 2004). Hardy et al. (2004) propose that $P2Y_{12}$ mediates inhibition of adenylate cyclase and activation of PI3K, which collectively positively modulates the $Ca^{2+}$ signal induced by ADP. The same $P2Y_1$-$P2Y_{12}$ crosstalk mechanism described in platelets by Hardy et al. (2004) was also suggested to be present in glioma C6 cells (Suplat et al., 2007).

The role of $P2Y_{12}$ in cells other than platelets is not well described, although recent evidence is promising. Findings by West et al. (2014) indicate a role for vessel wall $P2Y_{12}$ in early atherogenesis, rather than platelet $P2Y_{12}$. In addition to cardiovascular disease, $P2Y_{12}$ has potentially been implicated in immune responses to ADP in macrophages (Zhang et al., 2016) and dendritic cells (Ben Addi et al., 2010) in functions such as antigen uptake and chemotaxis. Therefore, non-platelet roles for $P2Y_{12}$ have been suggested and should be further investigated.

Monocytes are essential immune cells that, together with their progeny, facilitate innate immune defence via phagocytosis and cytokine production, but also activate the adaptive immune system through antigen uptake and presentation (Ziegler-Heitbrock, 2006). In this study, we apply the THP-1 monocytic cell line as an experimental model to investigate the expression of $P2Y_{12}$ and the contribution of the receptor in ADP-evoked $Ca^{2+}$ responses, exploring the signal transduction mechanisms involved. As there have been no publications reporting a role for $P2Y_{12}$ in monocytes, this investigation reveals a new role for $P2Y_{12}$ in non-platelet $Ca^{2+}$ responses, and contributes to our understanding of how monocytes function in health and disease.

## MATERIALS AND METHODS

### *Chemicals and reagents*

Unless otherwise stated, all chemicals and reagents were purchased from Sigma-Aldrich, with the exception of *pertussis toxin* and SQ22536 (Tocris). All chemicals (agonists and antagonists) were diluted using physiological saline (SBS buffer) (containing (mM): NaCl, 130; KCl, 5; MgCl2, 1.2; CaCl2, 1.5; D-glucose, 8; HEPES, 10; pH 7.4) with the exception of CCL2 (SBS buffer containing 1%(w/v) bovine serum albumin), MRS2578, SQ22536 and ticagrelor (SBS buffer containing 1% (v/v) DMSO).

### *Isolation of CD14$^+$ human monocytes*

Peripheral blood mononucleated cells (PBMCs) were isolated from the blood of human volunteers using Histopaque-1077 (Sigma-Aldrich). CD14+ monocytes were magnetically labelled from a PBMC suspension using MACS CD14 MicroBeads (Miltenyi Biotec), and positively selected for via the MACS Cell Separation Column (Miltenyi Biotec) together with the QuadroMACS Separator (Miltenyi Biotec).

### *Intracellular $Ca^{2+}$ measurements & drug treatments*

1 x $10^6$ THP-1 cells/mL were loaded for 1 h with 2 µM fura-2 AM in SBS buffer plus 0.01% (w/v) pluronic acid at 37°C. Cells were then pelleted and washed using SBS and plated at a density of 2x$10^5$ cells/well. The plated cells were allowed to settle for 1 hour at 37°C, during which stage antagonists were added 30 minutes into the hour, unless otherwise stated. Measurements were taken at 37°C using the FlexStation 3 instrument (Molecular Devices) measuring fura-2 fluorescence (340 nm excitation when $Ca^{2+}$-bound; 380 nm excitation when unbound; 510 nm emission) at intervals of 2 seconds giving. For all $Ca^{2+}$ experiments, the signal reported is 'F ratio', the ratio between Fura-2 emission at 510 when excited at 340 and 380nm. For hexokinase-treated of ADP stocks, 1mM ADP in SBS solution was treated for 1 hour at 37°C with 3 U/mL hexokinase from *Saccharomyces cerevisiae* (Sigma) prior to agonist application.

### *Cell culture*

Cells from the THP-1 cell line were cultured at 37°C, 5% $CO_2$ in RPMI 1640 medium containing 2 mM L-glutamine and supplemented with 10% (v/v) foetal bovine serum (FBS), 50 IU/mL penicillin and 50 µg/mL streptomycin. Cells were maintained at a density between 1 x $10^5$ and 1 x $10^6$ cells/mL.

### *siRNA-mediated gene knockdown*

THP-1 cells (2 x $10^5$ final amount) were incubated overnight in complete RPMI (10% FBS) without antibiotic before cells were transfected using Dharmacon siRNA (25 nM final concentration) via DharmaFECT 2 transfection reagent (obtained from Dharmacon Research, Inc.) using the manufacturer's protocol in 96-well format.

### *RNA extraction & RT-PCR*

Total RNA was extracted from THP-1 cells and CD14$^+$ monocytes using Tri reagent (Sigma Aldrich) with a subsequent DNase I treatment (Ambion). Complementary DNA was synthesised from 1 µg of total RNA using Superscript II reverse transcriptase (Invitrogen). PCR was performed using a Taq polymerase readymix (Sigma Aldrich) using primer pairs designed using the following sequences (accession numbers): *P2RY1* - GTTCAATTTGGCTCTGGCCG (5'-3'), TTTTGTTTTTGCGGACCCCG (3'-5') (NM_002563); *P2RY6* - GCTCTCACTGTCATCGGCTT (5'-3'), TCTGCCATTTGGCTGTGAGT (3'-5') (NM_176798); *P2RY12* - ACTGGGAACAGGACCACTGA (5'-3'), CAGAATTGGGGCACTTCAGC (3'-5') (NM_022788); *P2RY13* - TTCCCAGCCCTCTACACAGT (5'-3'), GGCCCCTTTAAGGAAGCACA (3'-5') (NM_176894).

***Immunocytochemistry***

THP-1 cells adhered to glass coverslips were washed twice in phosphate-buffered saline (PBS) followed by fixative with 4%(w/v) paraformaldehyde. Cells were permeabilised with 0.25%(v/v) triton X-100 for 10 minutes followed by blocking with 1%(w/v) bovine serum albumin (BSA) for 30 minutes at room temperature. Primary and secondary antibodies were diluted in PBS containing 1%(w/v) BSA and incubated with cells overnight a 4$^{O}$C and for 1 hour at room temperature, respectively. Cells were mounted in Vectashield containing nucleus counterstain (4',6-diamidino-2-phenylindole; DAPI). Goat polyclonal anti-$P2Y_{12}$ (Santa Cruz Biotechnology Inc) was used with Alexa 488-conjugated rabbit anti-goat (Abcam). Rabbit polyclonal anti-$P2Y_1$, anti-$P2Y_6$ and anti-$P2Y_{13}$ (Alomone) were used with Alexa 488-conjugated goat anti-rabbit (Invitrogen). Cell imaging was performed using a laser-scanning Zeiss LSM510 Meta confocal microscope.

*Transmigration assays*

Transwell migration assay were perfomed as previously described (Sivaramakrishnan et al., 2012; Campwala et al., 2014). Briefly, assays were performed in 24-well plates using polyethylene terephthalate (PET) membrane transwell inserts with 3 μm pores. 1x10$^6$ THP-1 cells in RPMI (no serum) with vehicle or drug treatment were added to the upper chamber, and 3 μM ADP or vehicle added to the lower chamber. Assays were performed for 2 hours at 37°C, and migrated cells counted on the underside of the transwell support using crystal violet staining. Chemotaxic index was calculated as the ration of cells that migrated to ADP over vehicle control.

***Data analysis***

Data analysis was performed using Origin Pro 9.0 software (Origin Lab, USA). Dose–response curves were fitted assuming a Hill coefficient of 1, with the Hill equation used to determine the degree of ligand-receptor cooperation. Figure data points represent mean values ± standard error of the mean (error bars). Statistical significance was determined using paired Student t-tests. Each point in the dose-response plots represents the average of the peak $Ca^{2+}$ response. A confidence interval of 5% ($P$<0.05) is used throughout for statement of significance.

Dose-response relationships were fitted using the equation of the hill equation:

$$response\ (y) = \frac{(\max - \min)}{1+10^{(\mathrm{Log\ EC50}-\mathrm{X})\mathrm{HillSlope}}}$$

**Nomenclature of Targets and Ligands**

Key protein targets and ligands in this article are hyperlinked to corresponding entries in http://www.guidetopharmacology.org, the common portal for data from the IUPHAR/BPS Guide to PHARMACOLOGY (Harding *et al.*, 2018), and are permanently archived in the Concise Guide to PHARMACOLOGY 2017/18 (Alexander *et al.*, 2017).

**RESULTS**

ADP-evoked intracellular $Ca^{2+}$ responses are mediated by $P2Y_6$ receptor activation and modulated by $G_i$-dependent signalling

ADP evoked concentration-dependent increases in intracellular $Ca^{2+}$ with a half-maximal concentration of 2.7±0.3 μM (N=5) (**Figures 1A and 1B**). Responses to maximal ADP concentrations were abolished following either phospholipase C inhibitor treatment (U73122) (**Figure 1C**) or calcium depletion of the ER store (thapsigargin) (**Figure 1D**). Study by Mahaut-Smith et al (2000) identified that commercially available ADP contains some ATP. To exclude any contribution of trace ATP to ADP-evoked $Ca^{2+}$ responses ADP stocks were treated with hexokinase. $Ca^{2+}$ response evoked by treated ADP were similar to untreated ADP, with a half-maximal concentration of 2.2 ±0.5 μM (N=5) (*P*>0.05 versus untreated ADP).

$P2Y_6$ antagonism by MRS2578 inhibited the ADP response almost completely with a half-maximal concentration of 200±20 nM (N=3) (**Figures 1E and 1F)**. MRS2578 inhibited the ADP response in a non-competitive fashion (**Figure 1G**), consistent with the reported mode of antagonism at $P2Y_6$ (Mamedova et al., 2004) and with previous findings (Sivaramakrishnan et al., 2012; Campwala et al., 2014). Selective inhibition of $P2Y_1$ with MRS2500 (tested up to 10 μM) (**Figure 1H**) or $P2Y_{13}$ with MRS2211 (tested up to 10 μM) (**Figure 1I**) had no significant effect of ADP evoked $Ca^{2+}$ responses. In addition to a dependency of phospholipase C activity and release of ER $Ca^{2+}$ stores, we investigated the effect of $G_i$-dependent signalling by using *Bordetella pertussis* toxin (PTx). PTx treatment (5 nM, 3 hours) caused a significant attenuation of ADP-evoked intracellular $Ca^{2+}$ response (**Figure 2A**), significantly suppressing the maximal response by approximately 30% and the half-maximal concentration for ADP ($EC_{50}$ 1.9±0.3 μM *vs* 2.9±0.2 μM with PTx; $p<0.05$, $N=5$) (**Figures 2B**). In control experiments, CCL2-evoked $Ca^{2+}$ responses were abolished by PTx treatment (**Figure 2C**), in agreement with our previous observations. Together these findings suggest that ADP-evoked $Ca^{2+}$ responses are mediated via $P2Y_6$ activation and release of ER $Ca^{2+}$, and that $G_i$-dependent signalling either constitutively or following ADP activation, positively modulates the ADP-evoked response.

We next determined the expression of ADP receptors in THP-1 cells in an effort to probe further the molecular basis of ADP-evoked $Ca^{2+}$ responses and identify receptors that may modulate them. RT-PCR analysis of P2Y receptors activated by ADP (Erb and Weisman, 2012; Communi et al., 1996) in THP-1 cells revealed expression of $P2Y_1$, $P2Y_6$, $P2Y_{12}$ and $P2Y_{13}$ (**Figure 3A**). $P2Y_{12}$ receptor mRNA expression was confirmed in freshly isolated $CD14^+$ monocytes (**Figure 3B**). $P2Y_1$, $P2Y_6$, $P2Y_{12}$ and $P2Y_{13}$ protein expression was confirmed by immunocytochemistry and confocal microscopy (**Figure 3C**).

Effect of $P2Y_{12}$ antagonism and knockdown on ADP-evoked $Ca^{2+}$ responses in THP-1 cells

Of the ADP receptors expressed by THP-1 monocytes, $P2Y_{12}$ is a known $G_i$-coupled receptor. The role of $P2Y_{12}$ activation during ADP challenge was investigated using PSB-0739, a high affinity competitive antagonist (Baqi et., 2009), and ticagrelor, a $P2Y_{12}$ antagonist used clinically as an anti-thrombotic agent (Husted et al., 2006). Ticagrelor inhibited ADP-evoked $Ca^{2+}$ responses in THP-1 cells in a concentration-dependent fashion (**Figure 4A**). Ticagrelor inhibited ADP-evoked $Ca^{2+}$ responses with a half-maximal concentration of 4.7±1.8 μM (*N*=5) and a non-competitive mode of action (**Figures 4B and 4C**). This is consistent with the observations of van Giezen et al (2009) where ticagrelor binds to $P2Y_{12}$ at a site distinct from that of ADP, producing a non-competitive inhibition of ADP-induced aggregation in human platelets. PSB-0739 inhibited ADP-evoked $Ca^{2+}$ responses with a half-maximal concentration of 5.4±1.8 μM (*N*=5) (**Figures 4D and 4E**) and caused a rightward parallel shift in the ADP concentration-response curve (**Figure 4F**). Inhibition of the ADP response was approximately 80% at the highest concentrations of PSB-0739 tested. Several studies have suggested that ticagrelor produces cardiovascular

benefit through a pleiotropic inhibition of the equilibrative nucleoside transporter 1 (ENT-1) (Aungraheeta et al., 2016), and a consequent elevation in extracellular adenosine. To rule out this mechanism of action in THP-1 cells, we inhibited ENT-1 using 3μM 6-*S*-[(4-nitrophenyl)methyl]-6-thioinosine (NBMPR), but observed no effect on ADP-evoked $Ca^{2+}$ responses (data not shown). Next, we undertook a gene knockdown strategy to support our observations with $P2Y_{12}$ receptor antagonists. siRNA targeting of $P2Y_{12}$ or control gene GADPH achieved approximately 40% mRNA knockdown versus scrambled siRNA control cells. ADP-evoked $Ca^{2+}$ responses were attenuated by approximately 30% in cells with $P2Y_{12}$ knockdown versus either GADPH knockdown or scrambled control cells (**Figures 4G and 4H**). To investigate the biological relevance of $P2Y_{12}$ receptor inhibition in THP-1s, we assays transmigration in response to ADP. In these experiments, ADP stimulated significant THP-1 transmigration over a 2 hour period over vehicle (**Figure 4I**). Addition of either ticagrelor or PSB-0739 attenuated cell migration to ADP (**Figure 4I).** Together these data reveal that $P2Y_{12}$ receptor activity is functional important for the generation of ADP evoked intracellular $Ca^{2+}$ responses and migration in THP-1 cells.

Adenylate cyclase inhibition reverses antagonistic effect of ticagrelor

We hypothesised that the molecular mechanism underlying the positive contribution of $P2Y_{12}$ receptor to ADP-evoked $Ca^{2+}$ responses could be due to a number of possibilities. Firstly, that $P2Y_{12}$ is solely $G_i$-coupled and its activity positively regulates $P2Y_6$-mediated $Ca^{2+}$ signalling through classical suppression of adenylate cyclase, or secondly that $P2Y_{12}$ can directly elicit a $Ca^{2+}$ response, either through promiscuous $G_q$ coupling or via $G_i$-coupling that directly elicits $Ca^{2+}$ signalling through activation of atypical phospholipase C, a for signalling on the CCL2-CCR2 axis (Myers et al., 1995). To explore this further, we investigated the requirement of adenylate cyclase activity for mediating the inhibitory action of ticagrelor. Adenylate cyclase inhibition with 300μM SQ22536 had no effect on ADP-evoked $Ca^{2+}$ responses (**Figure 5A**). However, SQ22536 could reverse the effect of ticagrelor, restoring the ADP concentration-response relationship and maximum response ($F_{max}$ = 3.32 ± 0.26 for ADP + 5 μM ticagrelor + 300 μM SQ22536; $F_{max}$ = 2.64 ± 0.21, ADP + 5 μM ticagrelor; $F_{max}$ = 1.06 ± 0.10; $N$=5. The $F_{max}$ for ADP + 5 μM ticagrelor *vs*. ADP + vehicle control is significantly different to $P$<0.05) (**Figures 5B and 5C**).

## DISCUSSION

Demonstrated in this study are novel findings identifying a role for $P2Y_{12}$ in regulating intracellular $Ca^{2+}$ signalling in non-platelet cells. We have utilised THP-1 cells, a model used extensively to investigate human monocyte function, to demonstrate a functional role for $P2Y_{12}$. In addition, we identify $P2Y_{12}$ expression in human $CD14^+$ monocytes. There have been no published reports on the expression of $P2Y_{12}$ in monocytes thus far, however the involvement of $P2Y_{12}$ function in macrophage was investigated by Kronlage et al (2010). Stimulation of $P2Y_{12}$ in macrophage was found to induce cell spreading with formation of lamellipodia, and inhibition of multiple purinergic receptors, including $P2Y_{12}$, attenuated chemotaxis (Kronlage et al., 2010). The signal transduction mechanisms downstream of $P2Y_{12}$ were not investigated in this study. $P2Y_{12}$ receptor expression has also been reported in glial cells, smooth muscle and endothelium (Cattaneo, 2007).

In this study, we demonstrate that ADP evokes intracellular $Ca^{2+}$ signalling via $P2Y_6$ receptor activation. $P2Y_6$ is often considered as the metabotropic receptor for UDP. Though UDP is a more potent agonist at the human $P2Y_6$ receptor by several orders of magnitude, ADP is a full agonist with a half-maximal concentration for inositol 1,4,5-triphosphate production in the micromolar range (Communi et al., 1996). ADP is an important signalling cue in monocyte/macrophage biology. For example, in the same cell-line used in this investigation, THP-1, ADP stimulation caused release of the cytokine tumour necrosis factor alpha (TNF-α) (Mattana et al., 2002). TNF-α release causes an inflammatory innate immune response

including immune cell recruitment. In addition, ADP has been shown in this investigation to induce calcium signals in THP-1 cells, and calcium signalling in circulating monocytes has in fact been suggested to result in the development of mature dendritic cells (Czerniecki et al., 1997). Such examples indicate that ADP contributes to monocyte function, with specific reference to immune responses and differentiation. ADP released from *E. coli*-infected mice, and from macrophages exposed to lipopolysaccharide (LPS), protected mice from E. coli-induced peritonitis via macrophage recruitment (Zhang et al., 2016). Additionally, ADP caused production of CCL2, a crucial chemokine in immune cell recruitment, which accordingly attracted more macrophages in a transwell assay (Zhang et al., 2016). Inhibition of downstream $P2Y_{12}$ signalling, or macrophage $P2Y_{12}$ deficiency, blocked immune responses to ADP, in turn allowing more bacteria to persist in infected mice (Zhang et al., 2016). This investigation by Zhang et al. revealed that upon sensing danger, macrophages release ADP, which binds to receptors such as $P2Y_{12}$, mediating actions such as chemokine release and consequent recruitment of immune cells. Such findings may implicate ADP and $P2Y_{12}$ as being crucial in forming a comprehensive immune response to infectious disease.

It was discovered in platelets by Hardy et al. (2004) that the selective pharmacological $P2Y_{12}$ inhibitor AR-C69931MX partially blocked the calcium response to 10 μM ADP, which was also shown to be completely abolished by selective $P2Y_1$ inhibition. This suggested that $P2Y_{12}$ is able to positively modulate the $P2Y_1$-mediated calcium response to ADP in platelets. Subsequently, Hardy et al. identified that the PI3K inhibitor LY294002 (10 μM) partially inhibited the $P2Y_{12}$-dependent part of the calcium response to ADP. Moreover, the adenylate cyclase inhibitor SQ22536 partially restored ADP-evoked calcium responses in the presence of the $P2Y_{12}$ inhibitor AR-C69931MX (Hardy et al., 2004). Taken together, these findings by Hardy et al. indicated in platelets that $P2Y_{12}$ regulates $P2Y_1$-mediated calcium responses to ADP through activation of PI3K and inhibition of adenylate cyclase. The findings in this investigation suggest that, of the ADP-activated P2Y receptors, ADP-induced calcium responses in THP-1 cells are dependent on $P2Y_{12}$ and $P2Y_6$ activation, but not dependent on $P2Y_1$ or $P2Y_{13}$. Therefore, the basic principle identified reported by Hardy et al. is supported here for THP-1 monocytic cells, only with $P2Y_6$ acting as the equivalent of $P2Y_1$.

Of interest is the observation that adenylate cyclase inhibition with SQ22536 on ADP-evoked $Ca^{2+}$ signals in the absence of $P2Y_{12}$ antagonism. This data suggests adenylate cyclase activity does not exert a suppressive effect when $P2Y_6$ and $P2Y_{12}$ concurrently activated by ADP. There are mechanistic explanations that could explain this observation. For example, there may be no net change in adenylate cyclase activity upon ADP challenge due to co-activation of a $G_i$-dependent pathway, mediated by $P2Y_{12}$, and a $G_s$-dependent pathway mediated by another ADP receptor or possible adenosine receptor. A predominance of $G_s$ signaling could be revealed following $P2Y_{12}$ inhibition, and increased adenylate cyclase activity suppresses ADP-evoked $Ca^{2+}$ signaling. Previous reports (Communi et al., 1997) have highlighted promiscuity for $G_s$ and $G_q$ coupling by $P2Y_{11}$ which is expressed by THP-1 cells (unpublished data). However, $P2Y_{11}$ is ATP activated and not activated by ADP at concentrations used in this study (Communi et al., 1997).

How might $P2Y_{12}$ regulate $P2Y_6$-dependent signaling via adenylate cyclase? Firstly, this is unlikely to involve PKA-dependent phosphorylation of the $P2Y_6$ receptor or receptor desensitization. Compared to other P2Y receptors, such as $P2Y_4$, $P2Y_6$ display limited reduction in cell surface receptor number even in the presence of maximal agonist concentrations (Brinson & Harden, 2000). There are no consensus PKA phosphorylation sites in the cytoplasmic loops of $P2Y_6$, though this cannot discount PKA phosphorylation of an auxillary protein that positively regulates $P2Y_6$ activity.

There is currently much interest in the biological effects of $P2Y_{12}$ antagonists beyond platelets (Nylander & Schultz, 2016). Although further work is required to investigate the role

of $P2Y_{12}$ in freshly isolated human monocytes, this work suggests that physiological and pharmacological modulation of $P2Y_{12}$ can influence ADP-evoked intracellular $Ca^{2+}$ signalling in THP-1 cells and perhaps monocytes, which will likely influence key monocyte functionality such as migration, adhesion and cytokine production.

**Author contributions**: JJM and JAL carried out the experiments and analysed the data. JJM, JAL and SJF designed the experiments and co-wrote the manuscript.

**Competing interests:** None

## REFERENCES


Alexander, S.P., Kelly, E., Marrion, N.V., Peters, J.A., Faccenda, E., Harding, S.D et al. (2017). The concise guide to pharmacology 2017/18. *British Journal of Pharmacology* Suppl 1: S1-S16.

Aungraheeta, R., Conibear, A., Butler, M., Kelly, E., Nylander, S., Mumford, A. et al. (2016). Inverse agonism at the P2Y12 receptor and ENT1 transporter blockade contribute to platelet inhibition by ticagrelor. *Blood*, 128(23), pp.2717-2728.

Baqi, Y., Atzler, K., Köse, M., Glänzel, M. and Müller, C. (2009). High-Affinity, Non-Nucleotide-Derived Competitive Antagonists of Platelet P2Y12Receptors. *Journal of Medicinal Chemistry*, 52(12), pp.3784-3793.

Ben Addi, A., Cammarata, D., Conley, P., Boeynaems, J. and Robaye, B. (2010). Role of the P2Y12 Receptor in the Modulation of Murine Dendritic Cell Function by ADP. *The Journal of Immunology*, 185(10), pp.5900-5906.

Brinson, A. and Harden, T. (2000). Differential Regulation of the Uridine Nucleotide-activated P2Y4 and P2Y6 Receptors. *Journal of Biological Chemistry*, 276(15), pp.11939-11948.

Campwala, H., Sexton, D., Crossman, D. and Fountain, SJ. (2014). P2Y6 receptor inhibition perturbs CCL2-evoked signalling in human monocytic and peripheral blood mononuclear cells. *Journal of Cell Science*, 127(22), pp.4964-4973.

Cattaneo, M. (2007). The Platelet P2 Receptors. *Platelets*, pp.201-220.

Communi, D., Govaerts, C., Parmentier, M. and Boeynaems, J. (1997). Cloning of a Human Purinergic P2Y Receptor Coupled to Phospholipase C and Adenylyl Cyclase. *Journal of Biological Chemistry*, 272(51), pp.31969-31973.

Communi, D., Parmentier, M. and Boeynaems, J. (1996). Cloning, Functional Expression and Tissue Distribution of the Human P2Y6 Receptor. *Biochemical and Biophysical Research Communications*, 222(2), pp.303-308.

Czerniecki, B., Carter, C., Rivoltini, L., Koski, G., Kim, H., Weng, D., et al. (1997). Calcium ionophore-treated peripheral blood monocytes and dendritic cells rapidly display characteristics of activated dendritic cells. *The Journal of Immunology*, 159(8), pp.3823-3837.

Dorsam, R. and Kunapuli, S. (2004). Central role of the P2Y12 receptor in platelet activation. *Journal of Clinical Investigation*, 113(3), pp.340-345.

Erb, L. and Weisman, G. (2012). Coupling of P2Y receptors to G proteins and other signaling pathways. *Wiley Interdisciplinary Reviews: Membrane Transport and Signaling*, 1(6), pp.789-803.

Harding SD, Sharman JL, Faccenda E, Southan C, Pawson AJ, Ireland S *et al.* (2018). The IUPHAR/BPS Guide to PHARMACOLOGY in 2018: updates and expansion to encompass the new guide to IMMUNOPHARMACOLOGY. Nucl Acids Res 46: D1091-D1106.

Hardy, A., Jones, M., Mundell, S. and Poole, A. (2004). Reciprocal cross-talk between P2Y1 and P2Y12 receptors at the level of calcium signaling in human platelets. *Blood*, 104(6), pp.1745-1752.

Husted, S., Emanuelsson, H., Heptinstall, S., Sandset, P., Wickens, M. and Peters, G. (2006). Pharmacodynamics, pharmacokinetics, and safety of the oral reversible P2Y12 antagonist AZD6140 with aspirin in patients with atherosclerosis: a double-blind comparison to clopidogrel with aspirin. *European Heart Journal*, 27(9), pp.1038-1047.

Jin, J. and Kunapuli, S. (1998). Coactivation of two different G protein-coupled receptors is essential for ADP-induced platelet aggregation. *Proceedings of the National Academy of Sciences*, 95(14), pp.8070-8074.

Kronlage, M., Song, J., Sorokin, L., Isfort, K., Schwerdtle, T., Leipziger, J et al. (2010). Autocrine Purinergic Receptor Signaling Is Essential for Macrophage Chemotaxis. *Science Signaling*, 3(132), pp.ra55-ra55.

Mahaut-Smith, M.P., Ennion, S.J., Rolf, M.G. and Evans, R.J (2000). ADP is not an agonist at P2X1 receptors: evidence for separate receptors stimulated by ATP and ADP on human plalets.

Mamedova, L., Joshi, B., Gao, Z., von Kügelgen, I. and Jacobson, K. (2004). Diisothiocyanate derivatives as potent, insurmountable antagonists of P2Y6 nucleotide receptors. *Biochemical Pharmacology*, 67(9), pp.1763-1770.

Mattana, A., Cappai, V., Alberti, L., Serra, C., Fiori, P. and Cappuccinelli, P. (2002). ADP and Other Metabolites Released from Acanthamoeba castellanii Lead to Human Monocytic Cell Death through Apoptosis and Stimulate the Secretion of Proinflammatory Cytokines. *Infection and Immunity*, 70(8), pp.4424-4432.

Myers, S., Wong, L. and Charo, I. (1995). Signal Transduction and Ligand Specificity of the Human Monocyte Chemoattractant Protein-1 Receptor in Transfected Embryonic Kidney Cells. *Journal of Biological Chemistry*, 270(11), pp.5786-5792.

Nylander, S. and Schulz, R. (2016). Effects of P2Y12receptor antagonists beyond platelet inhibition - comparison of ticagrelor with thienopyridines. *British Journal of Pharmacology*, 173(7), pp.1163-1178.

Sivaramakrishnan, V., Bidula, S., Campwala, H., Katikaneni, D. and Fountain, SJ. (2012). Constitutive lysosome exocytosis releases ATP and engages P2Y receptors in human monocytes. *Journal of Cell Science*, 125(19), pp.4567-4575.

Suplat, D., Krzemiński, P., Pomorski, P. and Barańska, J. (2007). P2Y1 and P2Y12 receptor cross-talk in calcium signalling: Evidence from nonstarved and long-term serum-deprived glioma C6 cells. *Purinergic Signalling*, 3(3), pp.221-230.

VAN GIEZEN, J., NILSSON, L., BERNTSSON, P., WISSING, B., GIORDANETTO, F., TOMLINSON, W. et al (2009). Ticagrelor binds to human P2Y12independently from ADP but antagonizes ADP-induced receptor signaling and platelet aggregation. *Journal of Thrombosis and Haemostasis*, 7(9), pp.1556-1565.

West, L., Steiner, T., Judge, H., Francis, S. and Storey, R. (2014). Vessel wall, not platelet, P2Y12 potentiates early atherogenesis. *Cardiovascular Research*, 102(3), pp.429-435.

Zhang, X., Qin, J., Zou, J., Lv, Z., Tan, B., Shi, J. et al (2016). Extracellular ADP facilitates monocyte recruitment in bacterial infection via ERK signaling. *Cellular & Molecular Immunology*.

Ziegler-Heitbrock, L. (2006). The CD14+ CD16+ blood monocytes: their role in infection and inflammation. *Journal of Leukocyte Biology*, 81(3), pp.584-592.

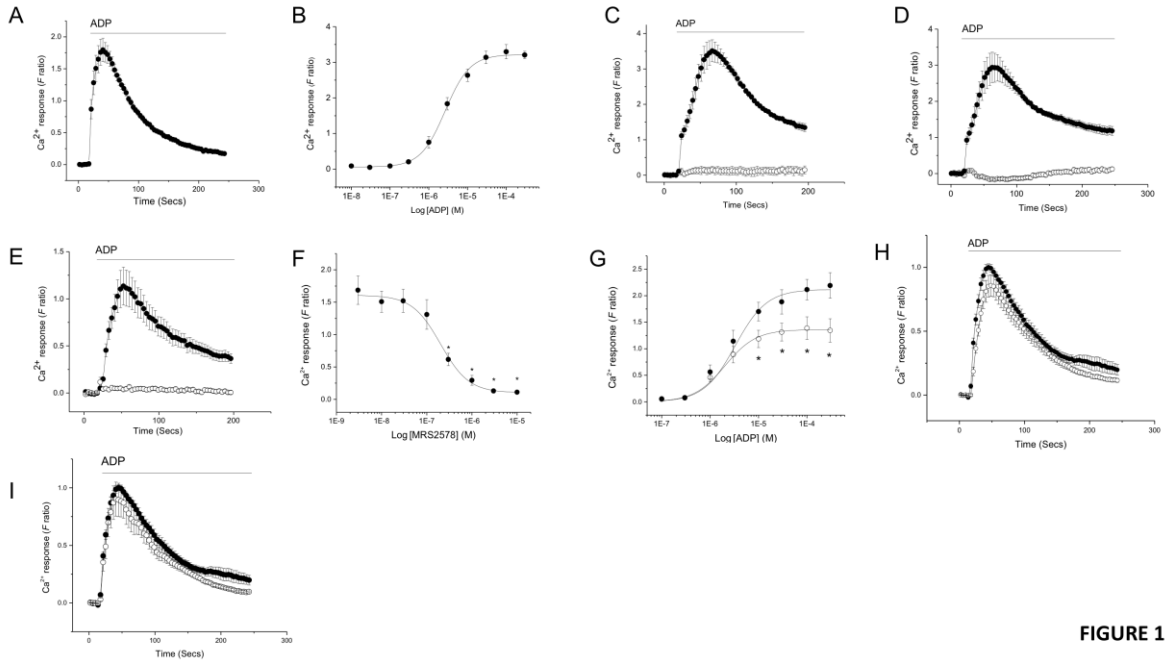


FIGURE 1

**Figure 1 $P2Y_6$ mediates ADP-evoked intracellular $Ca^{2+}$ responses in THP-1 cells**. (A) Averaged (*N*=5) intracellular $Ca^{2+}$ response evoked by ADP (30μM). (B) Concentration-dependency of ADP-evoked responses ($EC_{50}$ 2.7±0.3μM; *N*=5). Abolition of responses evoked by 30μM ADP in control conditions (*closed circles*) or following pre-incubation (*open circles*) with 5μM U73122 (C) or 1 μM Thapsigargin (D); *N*=5 for both. (E) ADP concentration response curve in the absence (*closed circles*) and presence (*open circles*) of 300nM MRS2578 (*N*=5). (F) Concentration-inhibition curve for $P2Y_6$ antagonist MRS2578 on intracellular $Ca^{2+}$ response evoked by ADP (3μM; *N*=5). (G) ADP concentration response curve in the absence (*closed circles*) and presence (*open circles*) of 300nM MRS2578 (*N*=5). (H and I) Averaged (*N*=5) intracellular $Ca^{2+}$ responses evoked by 3μM ADP in the presence of vehicle (*closed circles*) or in the presence of $P2Y_1$ antagonist 1μM MRS2500 (H; *open circles*) or $P2Y_{13}$ antagonist 10μM MRS2211 (I; *open circles*). For all experiments, *F* ratio is the ratiometric measurement of intracellular $Ca^{2+}$ using fura-2. * $p<0.05$

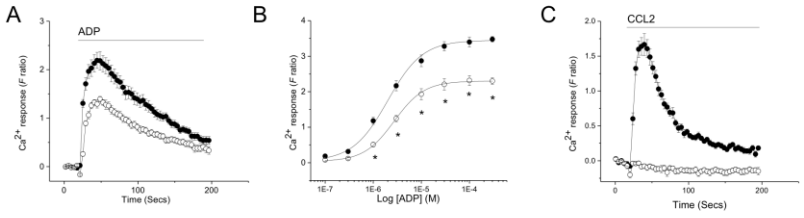


FIGURE 2

**Figure 2 Pertussis toxin attenuates ADP-evoked intracellular $Ca^{2+}$ responses in THP-1 cells.** (A) Averaged (*N*=5) intracellular $Ca^{2+}$ response evoked by ADP (3μM) in the absence (*closed circles*) and presence (*open circles*) of 5nM pertussis toxin (3 hr pre-incubation). (B) ADP concentration-response relationship in absence (*closed circles*) and presence (*open circles*) of 5nM pertussis toxin (*N*=5). (C) Positive control showing abolition of control CCL2-evoked response (*closed circle*) by 5nM pertussis toxin (*open circles*) (*N*=5). Responses evoked by 50ng/mL CCL2. For all experiments, *F* ratio is the ratiometric measurement of intracellular $Ca^{2+}$ using fura-2. * $p<0.05$.

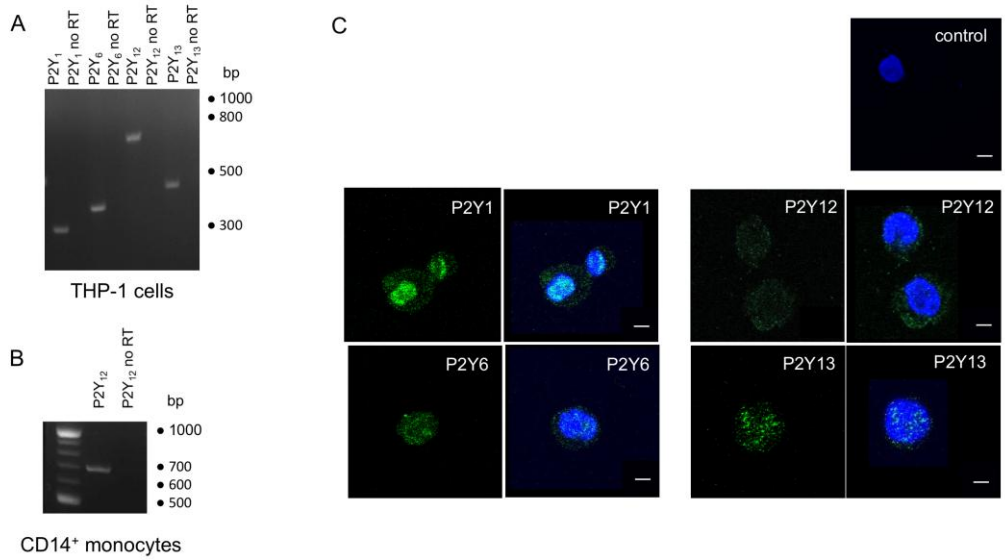


FIGURE 3

**Figure 3 Expression of ADP-activated P2Y receptors in THP-1 cells.** (A) RT-PCR analysis of $P2Y_1$ (326 bp), $P2Y_6$ (391 bp), $P2Y_{12}$ (698 bp) and $P2Y_{13}$ (461 bp) expression in THP-1 monocytes. RT-PCR analysis of $P2Y_{12}$ (698) expression in freshly isolated $CD14^+$ monocytes from human peripheral blood. For (A) and (B): predicted PCR ampilicon size given in parentheses; no RT (no reverse transcriptase) denotes negative control experiments for genomic DNA contamination. (C) Representative confocal microscopy images showing P2Y primary antibody immunoreactivity in fixed THP-1 cells. Cells are labelled with polyclonal antibodies against P2Y receptor subunits and fluorescence (*green*) visualised by using a AF488-conjugated secondary antibody (*lefthand panels*). *Control* is representative of an experiment where primary antibodies have been omitted. Cells are counterstained with diamidino-2-phenylindole to identify nuclei (*blue; in overlay in righthand panel*). Scale bar is 5μm. Experiments are representative of at least 3 independent experiments.

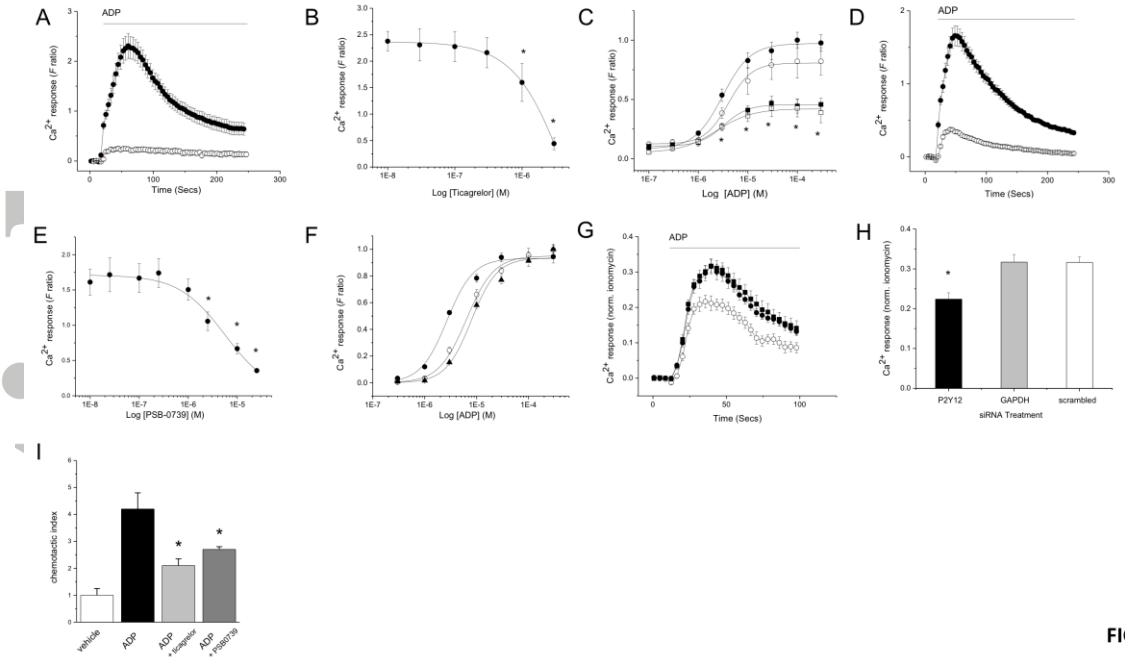


FIGURE 4

**Figure 4 Effect of $P2Y_{12}$ receptor antagonism and gene knockdown on ADP-evoked intracellular $Ca^{2+}$ responses in THP-1 cells.** (A) Averaged (*N*=5) ADP-evoked $Ca^{2+}$ response in the absence (*closed circles*) and presence (*open circles*) of 3μM ticagrelor. (B) Ticagrelor concentration-inhibition curve ($IC_{50}$ 4.7±1.8μM; *N*=5) for responses evoked by 3μM ADP. (C) ADP concentration-response curve (*N*=5) in the presence of vehicle (*closed circles*) or 0.1 (*open circles*), 1 (*closed squares*) and 5μM ticagrelor (*open squares*). (D) Averaged (*N*=5) ADP-evoked $Ca^{2+}$ response in the absence (*closed circles*) and presence (*open circles*) of 25μM PSB-0739. (E) PSB-0739 concentration-inhibition curve ($IC_{50}$ 5.4±1.8μM; *N*=5) for responses evoked by 3μM ADP. (F) ADP concentration response curve (*N*=4) in the presence of vehicle (*closed circles*) or 5 (*open circles*) and 10μM PSB-0739 (*closed triangles*). (G) Effect of siRNA-mediated silencing of $P2Y_{12}$ on ADP-evoked $Ca^{2+}$ responses. Averaged (*N*=5) $Ca^{2+}$ responses evoked by 3μM ADP in THP-1 cells following siRNA-mediated mRNA knockdown of $P2Y_{12}$ (*open circles*) or GAPDH (*closed squares*) compared to cells transfected with scrambled siRNA (*closed circles*) (*N*=5). (H) Bar chart showing effect of different siRNA treatment on peak $Ca^{2+}$ responses evoked by 3μM ADP (*N*=5). Responses in panels G and H are normalised to the magnitude of $Ca^{2+}$ response elicited by 100 μM ionomycin to control for cell number. For all experiments, *F* ratio is the ratiometric measurement of intracellular $Ca^{2+}$ using fura-2. * $p<0.05$ (I) $P2Y_{12}$ antagonists attenuate THP-1 transwell migration towards ADP. Chemotactic indexes comparing cell movement over 2 hours in control conditions (*vehicle*), 3μM ADP alone or in the presence of either ticagrelor (3μM) or PSB-0739 (25μM) (*$p<0.05$ versus ADP alone; *N*=5).

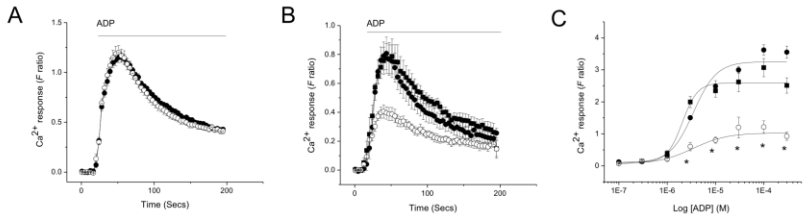


FIGURE 5

**Figure 5 Inhibition of adenylate cyclase reverses antagonistic action of ticagrelor on ADP-evoked $Ca^{2+}$ responses in THP-1 cells**. (A) Averaged *(N*=5) 3μM ADP-evoked $Ca^{2+}$ in the presence of vehicle *(closed circles*) or following adenylate cyclase inhibition with 300μM SQ22536. (B) Averaged *(N*=5) 3μM ADP-evoked $Ca^{2+}$ in the presence of vehicle *(closed circles*), 5μM ticagrelor (*open circles*) or 5μM ticagrelor plus 300μM SQ22536 (*closed squares*). (C) ADP concentration-response curve (*N*=5) in the presence of vehicle (*closed circles*), 5μM ticagrelor (*open circles*) or 5μM ticagrelor plus 300μM SQ22536 (*closed squares*). For all experiments, *F* ratio is the ratiometric measurement of intracellular $Ca^{2+}$ using fura-2. * $p<0.05$.